SUPPORTING INFORMATION

Photoresponsive Au_{25} Nanocluster Protected by Azobenzene Derivative Thiolates

Yuichi Negishi,*[ab] Ukyo Kamimura,[a] Mao Ide,[a] and Michiyo Hirayama[a]

[a]*Department of Applied Chemistry, Faculty of Science, Tokyo University of Science, 1-3 Kagurazaka, Shinjuku-ku, Tokyo 162-8601, Japan.*
[b]*Research Institute for Science and Technology, Energy and Environment Photocatalyst Research Division, Tokyo University of Science, 1-3 Kagurazaka, Shinjuku-ku, Tokyo 162-8601, Japan.*

A. Chemicals

All chemicals were commercially obtained and used without further purification. Hydrogen tetrachloroaurate tetrahydrate ($HAuCl_4 \cdot 4H_2O$) was obtained from Tanaka Kikinzoku. Sodium tetrahydroborate ($NaBH_4$), magnesium sulfate ($MgSO_4$), thioacetic acid (CH_3COSH), sodium hydroxide (NaOH), methanol, chloroform, hexane, dichloromethane, and toluene were purchased from Wako Pure Chemical Industries. 4-(phenylazo)phenol, sodium hydride (NaH), and 1,4-dibromobutane ($Br(CH_2)_4Br$) were purchased from Tokyo Kasei. *N*, *N*-dimethylformamide, ethylacetate, potassium carbonate (K_2CO_3), silica gel 60N, and tetrahydrofuran were purchased from Kanto Kagaku. *Trans*-2-3-[3-(4-*tert*-butylphenyl)-2-methyl-2-propenylidene]-malononitril (DCTB) was purchased from Furuka. Deionized water with a resistivity of >18.2 MΩ cm was used.

B. Synthesis of 4-(4-(phenylazo)phenoxy)butyl-1-thiol (Az–SH)

Az–SH was synthesized from 4-(phenylazo)phenol(**1**) by the following three steps (Scheme S1).

Step 1: Esterification of the hydroxyl group

First, 2.0 g of **1** was dissolved in 100 mL of *N*,*N*-dimethylformamide. To this solution, 15 mmol of NaH was added and the solution was stirred for 5 min. Then, 15 mmol of $Br(CH_2)_4Br$ was added to this solution. The solution was stirred for 1 h. Then, 100 mL of saturated ammonium chloride was added to the solution to stop the reaction and ethyl acetate was added, causing the solution to separate into two layers. The organic phase was separated from the solution and washed with water. After removing the water from the organic phase using $MgSO_4$, the organic phase was evaporated to dryness to obtain **2** (Scheme S1).

Step 2: Thioacetylation of the bromo group

First, 15 mmol of CH_3COSH was dissolved in 30 mL of *N*,*N*-dimethylformamide. To this solution, 15 mmol of NaH was added and the solution was stirred for 5 min. Then, 70 mL of *N*,*N*-dimethylformamide containing **2** was added to this solution and the solution was stirred for 50 min. Then, 100 mL of saturated ammonium chloride was added to the solution to stop the reaction and ethyl acetate was added, causing the solution to separate into two layers. The organic phase was separated from the solution and washed with a 1.0 M NaOH aqueous solution. After removing the water from the organic phase using $MgSO_4$, the organic phase was evaporated to dryness to obtain **3** (Scheme S1).

Step 3: Hydrolysis of the thioacetyl group

First, **3** was dissolved in 20 mL of chloroform. To this solution, 100 mL of methanol and 15.0 mmol of K_2CO_3 were added. The solution was stirred for 1 h. Then, 100 mL of saturated ammonium chloride was added to the solution to stop the reaction and chloroform was added, causing the solution to separate into two layers. The organic phase was separated

from the solution and washed with water. After removing the water from the organic phase using $MgSO_4$, the organic phase was evaporated to dryness. The product was subsequently dissolved in a small quantity of chloroform and the target Az–SH was separated by chromatography (filling material: silica gel 60 N; eluent solvent: 5:1 hexane:ethyl acetate). The yield of Az–SH from 4-(phenylazo)phenol was 48.6%.

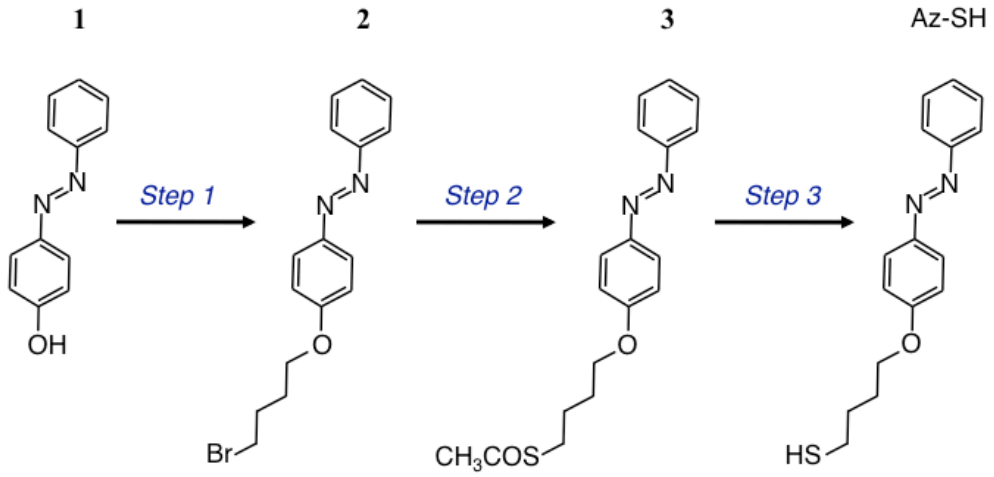

Scheme S1. Synthesis of Az–SH

C. Estimation of photoisomerization efficiency

C.1. Isomerization from *trans* to *cis* conformation

Almost all the Az–SH that is not ligated to a cluster isomerizes in toluene solution. Figure 3(a) shows that the absorption at 3.54 eV decreases to 10% on such isomerization. The absorbance attributable to S–Az in the absorption spectrum of $[Au_{25}(S–Az)_{18}]^-$ could be estimated by subtracting the absorption spectrum of $[Au_{25}(SC_2H_4Ph)_{18}]^-$ from that of $[Au_{25}(S–Az)_{18}]^-$. We estimate the absorbance attributed to S–Az at 3.54 eV in the spectra obtained before and after UV irradiation. We compared the absorbances at this energy of both spectra. It was found that UV irradiation reduces the absorbance attributed to S–Az to approximately 10%. This suggests that almost all the S–Az isomerizes from the *trans* to *cis* conformation, even in $[Au_{25}(S–Az)_{18}]^-$.

C.2. Isomerization from *cis* to *trans* conformation

Figure 3(b) shows that the absorbance attributed to S–Az at 3.54 eV is recovered up to approximately 97% on visible light irradiation. This suggests that almost all the S–Az isomerizes also for the isomerization from the *cis* to *trans* conformation.

D. Results

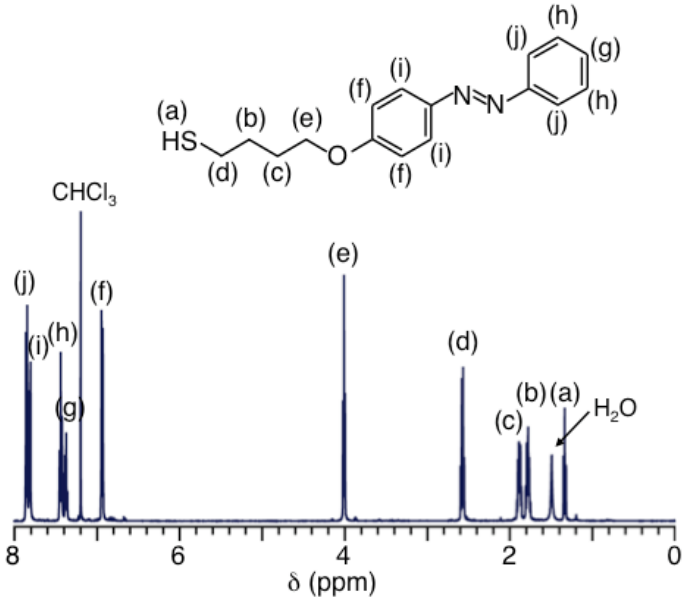

Figure S1. ^{1}H nuclear magnetic resonance (NMR) spectrum of Az–SH. NMR analysis was conducted on a JEOL JNM-LA500 spectrometer. The data was collected with a sample in $CDCl_3$. NMR assignment was performed based on data in the literature[1].

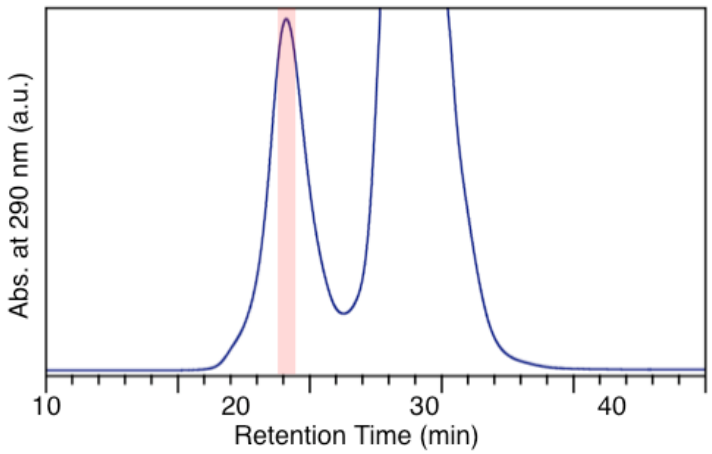

Figure S2. Chromatogram of as-prepared clusters. In this experiment, a high-performance liquid chromatography (HPLC) system (Japan Analytical Industry Co., Ltd., LC-9201) equipped with a stainless-steel column (Waters Co., Ultrastyragel^{TM}) was used to separate the objective cluster. Toluene was used as the eluent with a flow rate of 2.4 mL/min. The UV–vis absorbance detector was operated at 290 nm.

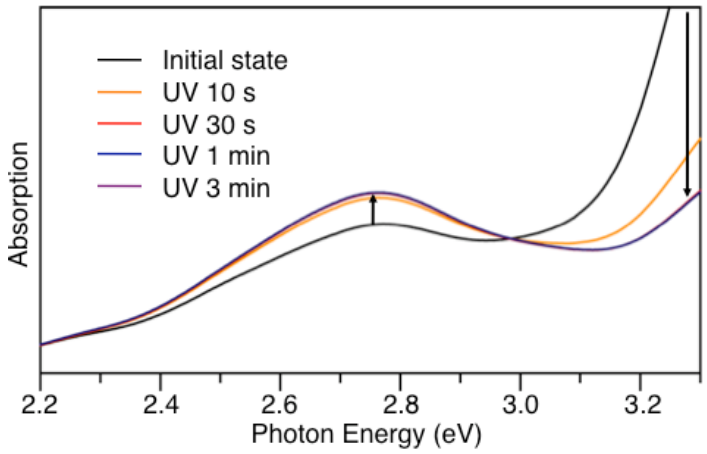

Figure S3. Photoresponsive behavior of the optical absorption spectrum of $[Au_{25}(S–Az)_{18}]^-$ toluene solution in the energy range 2.2–3.3 eV. The spectra overlap each other after 30 s, indicating that this photoreaction saturates at 30 s.

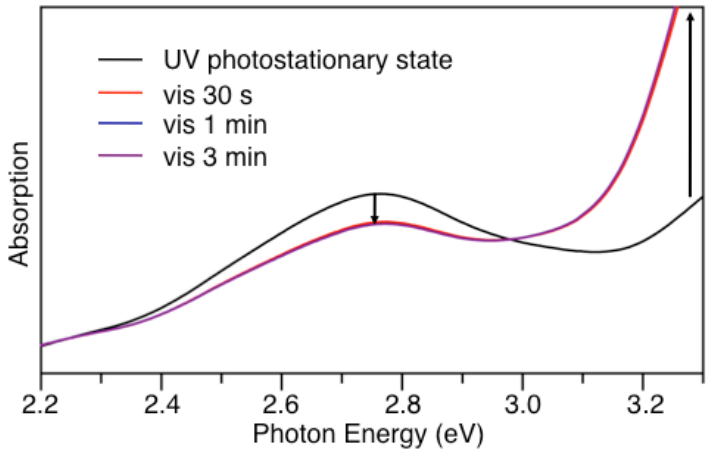

Figure S4. Photoresponsive behavior of optical absorption spectrum of $[Au_{25}(S–Az)_{18}]^-$ toluene solution in the energy range 2.2–3.3 eV. The spectra overlap each other after 30 s, indicating that this photoreaction saturates at 30 s.

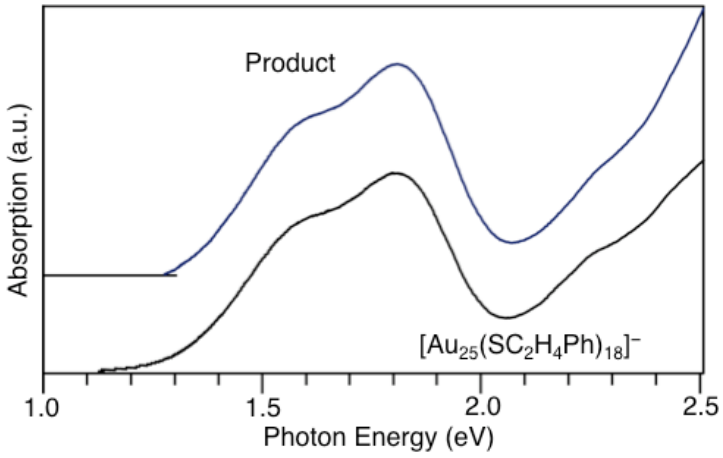

Figure S5. Optical absorption spectrum of toluene solution of the product together with that of $[Au_{25}(SC_2H_4Ph)_{18}]^-$ [2–4] for comparison.

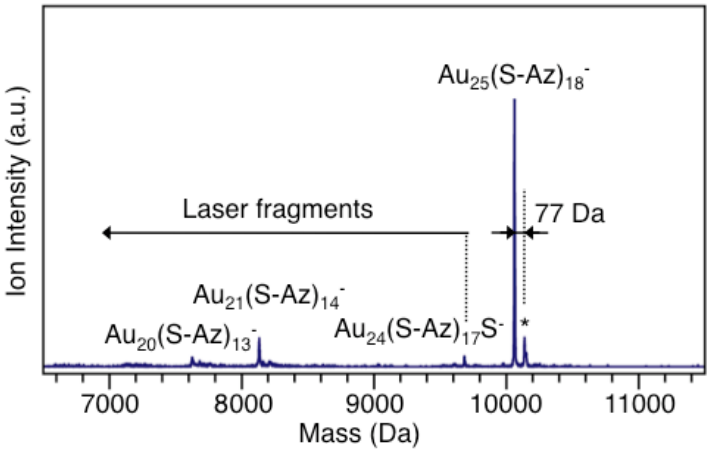

Figure S6. Enlarged MALDI mass spectrum of the products. The peak indicated by the asterisk is assigned to $[Au_{25}(S–Az)_{18}]^-$ accompanying the phenyl radical, which is probably a laser fragment of the product.

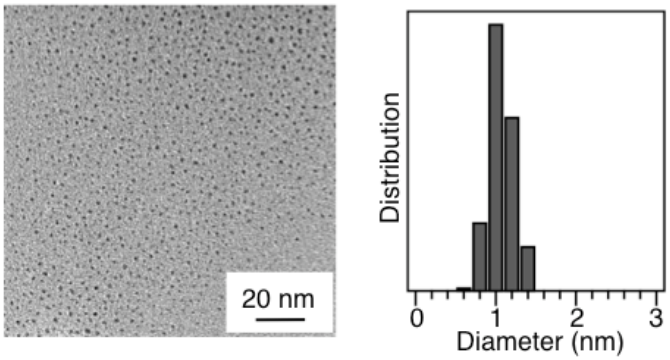

Figure S7. TEM image and core size distribution of the product. The core diameter of the product is 1.0 ± 0.2 nm.

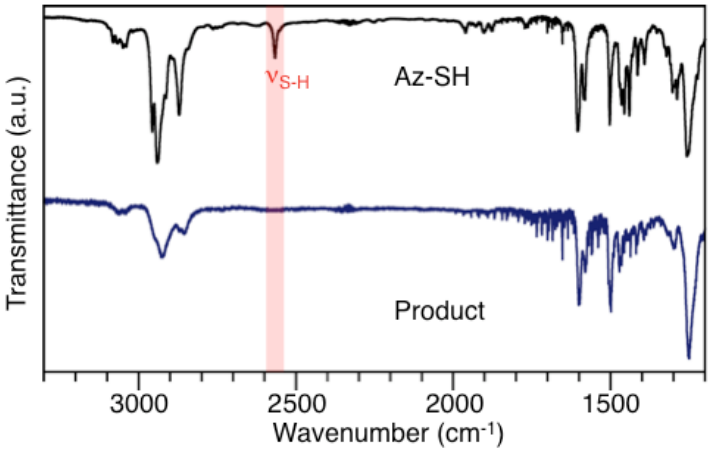

Figure S8. FT-IR spectra of Az–SH and the product.

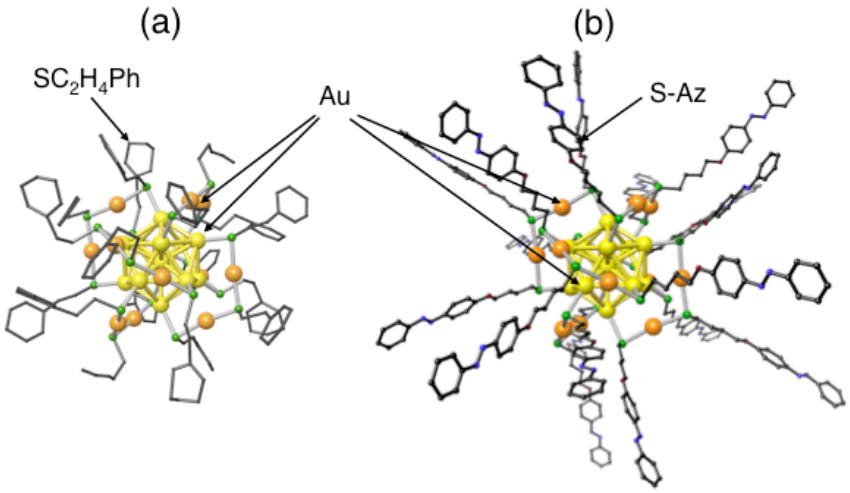

Figure S9. (a) Structural representation of $[Au_{25}(SC_2H_4Ph)_{18}]^-$.[5,6] (b) Proposed structure for $[Au_{25}(S–Az)_{18}]^-$.

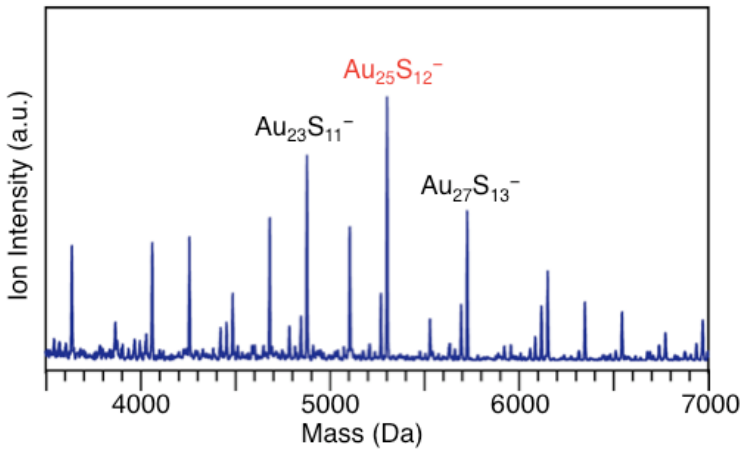

Figure S10. Negative-ion LDI mass spectrum of $[Au_{25}(SC_2H_4Ph)_{18}]^-$.[7] The most intense peak is $Au_{25}S_{12}^-$, which is formed by the desorption of six S atoms and C–S dissociation. The LDI mass spectrum (laser dissociation pattern) of $[Au_{25}(S–Az)_{18}]^-$ (Figure 2(a)) is highly consistent with this spectrum (laser dissociation pattern).

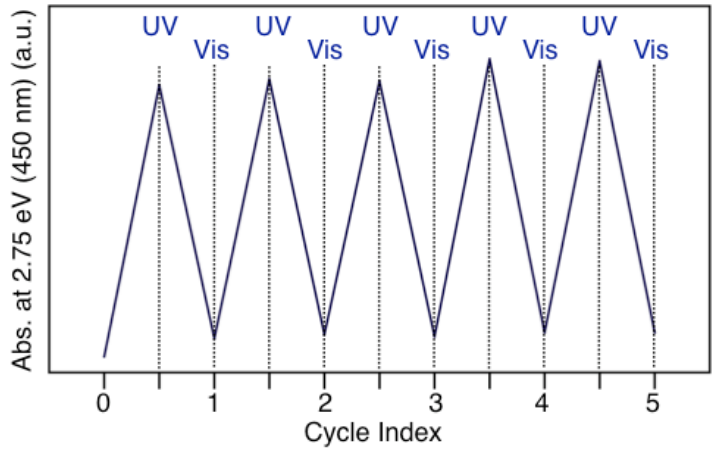

Figure S11. Changes in the absorbance of the toluene solution of $[Au_{25}(S–Az)_{18}]^-$ at 2.75 eV on photoirradiation with UV and visible light.

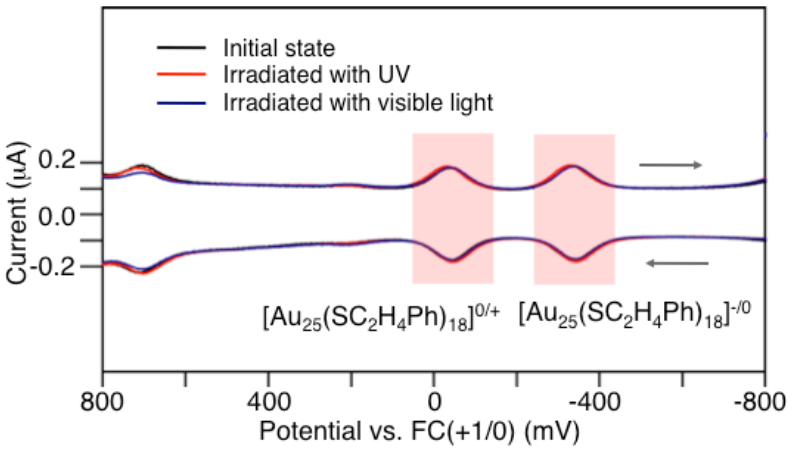

Figure S12. Photoresponsive behavior of differential pulse voltammogram (DPV) of $[Au_{25}(SC_2H_4Ph)_{18}]^-$. In this experiment, the toluene solution of $[Au_{25}(C_2H_4Ph)_{18}]^-$ was first irradiated by UV and then by visible light. After photoirradiation, the photoproducts were evaporated to dryness and were dissolved in 0.1 M $(C_4H_9)_4NPF_6$ CH_2Cl_2 solution. DPV was performed at room temperature. In contrast to the voltammogram of $[Au_{25}(S–Az)_{18}]^-$, that of $[Au_{25}(SC_2H_4Ph)_{18}]^-$ does not change on photoirradiation.

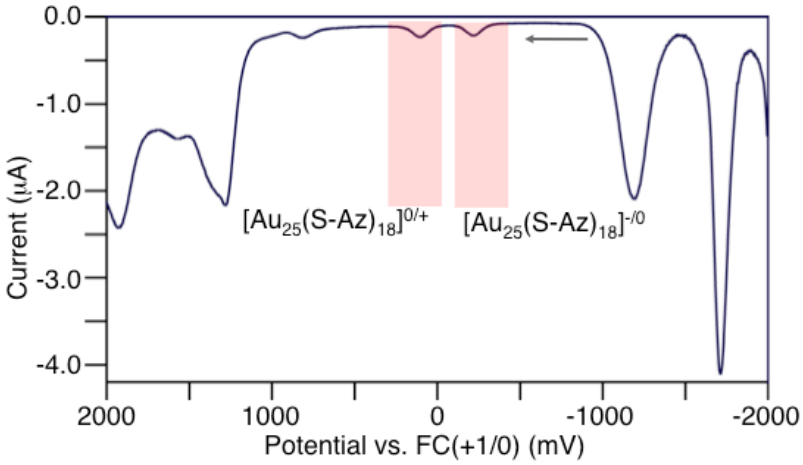

Figure S13. Differential pulse voltammogram (DPV) curve for $[Au_{25}(S–Az)_{18}]^-$ obtained before photoirradiation (scanning in the positive direction only). In the potential range –1000 to 1000 mV, the voltammogram has a very similar profile to that of $[Au_{25}(C_2H_4Ph)_{18}]^-$ (Figure S12 and Refs. 8–11). Therefore, the peaks at –206 and 126 mV are attributed to peaks derived from the redox potentials of $[Au_{25}(S–Az)_{18}]^{-1/0}$ and $[Au_{25}(S–Az)_{18}]^{0/+1}$, respectively; these peaks are not observed in the DPV curve of Az–SH (Figure S14). The assignments of the other peaks are currently under consideration.

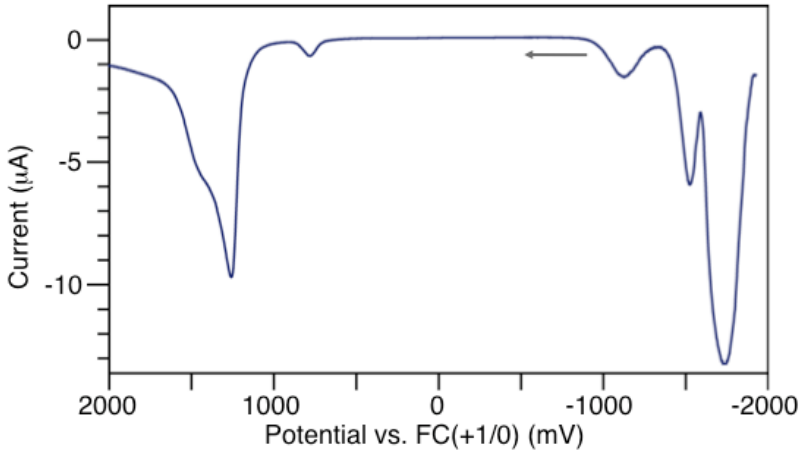

Figure S14. Differential pulse voltammogram (DPV) curve for Az–SH (scanning in the positive direction only). The peaks were not observed in the potential range of –800 to 800 mV, supporting the above assignments of the peaks at –206 and 126 mV observed in the DPV curve of $[Au_{25}(S–Az)_{18}]^-$ to peaks derived from the redox potentials of $[Au_{25}(S–Az)_{18}]^{-1/0}$ and $[Au_{25}(S–Az)_{18}]^{0/+1}$, respectively (Figure S13).

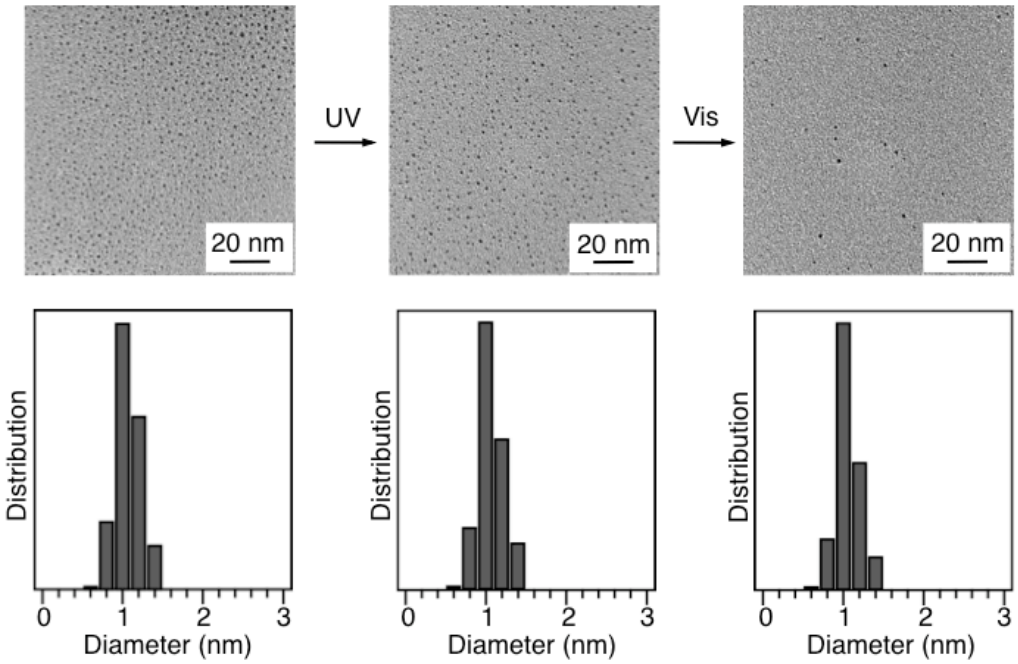

Figure S15. TEM images and core size distributions of $[Au_{25}(S–Az)_{18}]^-$ obtained before and after photoirradiation. $[Au_{25}(S–Az)_{18}]^-$ was irradiated first by UV and then by visible light in toluene solution.

References

1. W.-W Zhang, X.-M. Ren, H.-F. Li, C.-S. Lu, C.-J. Hu, H.-Z. Zhu and Q.-J. Meng, *J. Colloid Interface Sci.,* 2002, **255**, 150–157.
2. D. Lee, R. L. Donkers, G. Wang, A. S. Harper and R. W. Murray, *J. Am. Chem. Soc.*, 2004, **126**, 6193–6199.
3. R. Guo and R. W. Murray, *J. Am. Chem. Soc.*, 2005, **127**, 12140–12143.
4. M. Zhu, E. Lanni, N. Garg, M. E. Bier and R. Jin, *J. Am. Chem. Soc.*, 2008, **130**, 1138–1139.
5. M. W. Heaven, A. Dass, P. S. White, K. M. Holt and R. W. Murray, *J. Am. Chem. Soc.*, 2008, **130**, 3754–3755.
6. M. Zhu, C. M. Aikens, F. J. Hollander, G. C. Schatz and R. Jin, *J. Am. Chem. Soc.*, 2008, **130**, 5883–5885.
7. Z. Wu, C. Gayathri, R. R. Gil and R. Jin, *J. Am. Chem. Soc.*, 2009, **131**, 6535–6542.
8. D. Lee, R. L. Donkers, G. Wang, A. S. Harper and R. W. Murray, *J. Am. Chem. Soc.*, 2004, **126**, 6193–6199.
9. R. Guo and R. W. Murray, *J. Am. Chem. Soc.*, 2005, **127**, 12140–12143.
10. J.-P. Choi, C. A. Fields-Zinna, R. L. Stiles, R. Balasubramanian, A. D. Douglas, M. C. Crowe and R. W. Murray, *J. Phys. Chem. C*, 2010, **114**, 15890–15896.
11. Z. Wu and R. Jin, *Nano. Lett.*, 2010, **10**, 2568–2573.